

TAKING ACCOUNT OF CYLINDRICAL SHAPE IN THE THEORY  
OF AN INDUCTIVE MHD PROPULSION UNIT WITH A FREE FIELD

T. A. Pupykina and V. I. Yakovlev

UDC 538.4

Inductive MHD propulsion units have been studied in [1, 2]. In [2] it was shown that the integral energy characteristics of a real MHD propulsion unit of finite dimensions differ qualitatively from the characteristics [1] obtained on an ideal model of it with an infinitely long cylindrical inductor, which creates a traveling wave with fixed frequency and phase velocity. The physical reason for this difference is that the source of the electromagnetic fields (the inductor) of a propulsion unit of finite dimensions creates a spectrum of waves which possess various phase velocities (and wave numbers), including waves with arbitrarily large velocities. The contribution made by the electromagnetic fields associated with these waves to the integral quantities (the thrust and the necessary electrical power) of the propulsion unit determines the peculiarity observed [2] in the behavior of the investigated characteristics. In this connection, there is one circumstance which may cast doubt on the usability of the qualitative results of [2], obtained on a model of a flat plate, to real devices which may be regarded as axially symmetric. The reason is the following: in the case of a flat plate the fields  $\mathbf{E}_k, \mathbf{H}_k$  in the liquid, which correspond to the spectral components of the current in the source, are proportional to the spectral component for all  $k$  and extend to distances  $\sim 1/k$  from the plane of the plate. In an axially symmetric device the  $z$ -component of the field  $\mathbf{H}$  (which determines the energy loss), for  $k \sim 0$ , is essentially enclosed within the source (within the "solenoid") and is small in the surrounding liquid; therefore in this case the contribution made by the neighborhood of the point  $k = 0$  to the integral energy characteristics must be substantially lower than in the case of a flat plate, and this fact may in principle lead to a qualitative difference between the results of the present study and the results of [2]. Accordingly, it is naturally of interest to investigate the energy characteristics with a more realistic axially symmetric model.

1. This study is devoted to the investigation of the energy characteristics of an axially symmetric inductive MHD propulsion unit with a free field (Fig. 1). It is assumed that the propulsion section consists of cylinder of radius  $R$  and length  $a$ , and attached to the propulsion section on each side is a cylindrical segment with a nonconducting surface, whose length is not less than the radius  $R$ . Under these conditions, we can calculate the electromagnetic quantities by using a scheme with an infinite cylinder, part of which (of length  $a$ ) is the propulsion unit, while the rest of its surface is made of a nonconductive material.

The source creating the electromagnetic field in the surrounding liquid (the inductor) creates surface currents which are given in the form of a traveling wave; these are distributed along the surface of the cylinder within the limits of the propulsion section. Using the dimensionless cylindrical coordinates  $r, \alpha, z$  (as our scale of length we take the dimension  $a$  of the propulsion section), we can state the distribution of the current as follows:

$$i_\alpha(r, z, t) = \operatorname{Re} J_0 i_1(z) e^{i(k_0 z - \omega_0 t)}, \quad (1.1)$$

$$i_1(z) = \begin{cases} i_0(z) & \text{for } |z| \leq 1/2, \\ 0 & \text{for } |z| > 1/2, \end{cases}$$

where  $J_0$  is the maximum current density;  $i_0(z)$  is a function characterizing the distribution of current amplitude over the propulsion section, with  $|i_0(z)|_{\max} = 1$ ; the dimensionless wave number  $k_0 = (2\pi/\lambda)a = n\pi$  determines the number  $n$  of half-waves  $\lambda/2$  of the current (1.1) that fit into the propulsion segment. The actual current distribution (1.1) is a superposition of an infinite set of waves propagated along the  $z$  axis. To see this, we note that, using the Fourier transform

$$i_1(z) = \int_{-\infty}^{\infty} i(k) e^{ikh} dk, \quad i(k) = \frac{1}{2\pi} \int_{-1/2}^{1/2} i_0(z) e^{-ikh} dz,$$

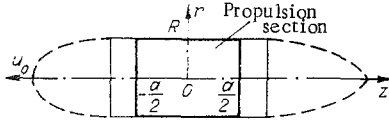


Fig. 1

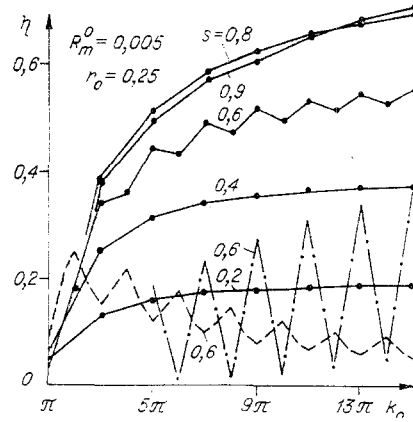


Fig. 2

we can represent the distribution (1.1) in the form

$$i_a(r, z, t) = \text{Re} J_0 \int_{-\infty}^{\infty} i(k - k_0) e^{ikz} dk e^{-i\omega_0 t}. \quad (1.2)$$

From this it can be seen that the components of the wave have a fixed frequency  $\omega_0$  and different phase velocities

$$v_p = v_p^0 \frac{k_0}{k},$$

which vary from  $-\infty$  to  $\infty$ . Here the subscript 0 denotes a fixed phase velocity

$$v_p^0 = \omega_0 a / k_0,$$

determined by the dimensional frequency  $\omega_0$  and the number  $k_0$ .

2. The distribution of the electric field  $\mathbf{E}$  and the magnetic field  $\mathbf{H}$  in the liquid (region 1) and within the cylinder (region 2) can be found, as in [2], on the assumption that the parameter of the MHD interaction is small; in Maxwell's equations, we use as the field of velocities of the liquid (with respect to the propulsion unit)  $\mathbf{v} = u_0 \mathbf{e}_z$ , where  $u_0$  is the velocity of motion of the body under consideration with respect to the liquid (see Fig. 1).

The vector potential describing the fields  $\mathbf{E}$ ,  $\mathbf{H}$  in the system under consideration will naturally be sought as the sum of waves similar to (1.2), i.e., in the form

$$\mathbf{A}_{1,2} = \frac{J_0 a}{c} \int_{-\infty}^{\infty} A_{1,2}(r, k) e^{ikz} dk e^{-i\omega_0 t} \mathbf{e}_z. \quad (2.1)$$

Then the equations for the dimensionless Fourier components  $A_{1,2}(r, k)$  (the subscripts indicate the number of the region), which follow from Maxwell's equations, can be reduced by using the independent variables  $\xi_{1,2} = \mu_{1,2} r$  [ $\mu_1 = i\sqrt{k^2 - iR_m(k_0 - ks)}$ ,  $\mu_2 = |k|$ ] to the Bessel equation

$$\frac{d^2 A_{1,2}}{d\xi_{1,2}^2} + \frac{1}{\xi_{1,2}} \frac{dA_{1,2}}{d\xi_{1,2}} + \left(1 - \frac{1}{\xi_{1,2}^2}\right) A_{1,2} = 0.$$

The solutions possessing the necessary properties for  $r = 0$  and  $r = \infty$  have the form

$$A_1(r, k) = C_1 H_1^{(1)}(i r \sqrt{k^2 - i R_m(k_0 - ks)}), \quad A_2(r, k) = C_2 I_1(|k| r). \quad (2.2)$$

Here  $H_1^{(1)}$ ,  $I_1$  are the Hankel function and the modified Bessel function, the expression  $\sqrt{k^2 - i R_m(k_0 - ks)}$  is taken to be a value with a positive real part, and the parameters ( $s$  is the slippage,  $R_m$  is the magnetic Reynolds number) are equal to

$$s = u_0 / v_p^0, \quad R_m = 4\pi\sigma v_p^0 a / c^2.$$

The arbitrary constants  $C_1$ ,  $C_2$  are determined from the conditions at the boundary  $r = R/a = r_0$ , which can be written in the form

$$(dA_1/dr - dA_2/dr)|_{r=r_0} = -4\pi i(k - k_0), \quad A_1(k, r_0) = A_2(k, r_0).$$

3. The integral quantities – the thrust created by the propulsion unit and the necessary electrical power – can be calculated as in [2], and the result for time-averaged quantities (over the period  $2\pi/\omega_0$ ) has the form

$$\langle F_z \rangle = -2\pi R \frac{H_0^2 a^2}{8\pi^2} R_m^0 F_1(k_0, r_0, R_m, s), \quad \langle Q \rangle = 2\pi R \frac{\omega_0 H_0^2 a^2}{8\pi^2} R_m^0 Q_1(k_0, r_0, R_m, s); \quad (3.1)$$

$$F_1 = \frac{8\pi^2}{R_m^0} \int_{-\infty}^{\infty} k \Phi(k) |i(k - k_0)|^2 dk, \quad Q_1 = \frac{8\pi^2}{R_m^0} \int_{-\infty}^{\infty} \Phi(k) |i(k - k_0)|^2 dk; \quad (3.2)$$

$$\Phi(k) = \text{Re} \frac{-iH_1^{(1)}(\mu_1 r_0) I_1(|k|r_0)}{|k| H_1^{(1)}(\mu_1 r_0) I_0(|k|r_0) - \mu_1 H_0^{(1)}(\mu_1 r_0) I_1(|k|r_0)}; \quad (3.3)$$

$$H_0 = 2\pi J_0/c. \quad (3.4)$$

The efficiency, defined as the ratio of the useful power  $|\langle F_z \rangle| u_0$  to the power actually used  $\langle Q \rangle$ , is equal to

$$\eta = \frac{s}{k_0} \frac{F_1}{Q_1}.$$

For comparison, we shall need the results relating to the case  $r_0 = \infty$ . These results can be obtained more easily not by writing out a general solution valid for arbitrary  $r_0$  but by directly considering a problem similar to [2] with the difference that the conductive liquid fills a half-space on one side of the plane of the plate, rather than the entire space as in [2]. The result is the following: the force and the electrical power per unit length of the plate are given by Eqs. (3.1) if we eliminate the factor  $2\pi R$  from them, and the dimensionless quantities  $F_1, Q_1$  are given by Eqs. (3.2) if we replace the function  $\Phi$  with

$$\Phi_0 = \text{Re} \frac{i}{|k| + \sqrt{k^2 + i R_m (k_0 - ks)}}. \quad (3.5)$$

It should be noted that in (3.1), (3.2) the quantity  $R_m^0 = R_m s$  denotes the magnetic Reynolds number, determined from the velocity  $u_0$ .

4. In [2] there was a qualitative investigation of the integral quantities similar to (3.2), and it was shown that the main contribution to the integrals is made by the neighborhoods of the points  $k = 0$  and  $k = k_0$ ; it is precisely the effect of the neighborhood of the point  $k = 0$  that causes the differences between the behavior of an MHD system with finite dimensions and that of an ideal system. Physically the contribution of this neighborhood means the contribution of the component waves which have high velocity (in comparison to  $v_p^0$ ) and move both in the positive and in the negative direction. Their contribution to the integral quantities leads to a decrease in the effectiveness of the system under consideration below the value for the ideal system. It was shown that the relative weight of these waves can be decreased by amplitude modulation, leading to a narrowing of the  $i(k)$  spectrum, and consequently to a reduction of the amplitudes of the waves which have phase velocities of large modulus.

In the cylindrical geometry considered here, the contribution of the "fast" waves to the required electrical field is much less than in the case of a flat plate. The reason is that the  $z$  component of the field  $\mathbf{H}$  in the liquid, which determines the radial component of the Poynting vector, is small for small values of  $|k|$  [this follows from (2.2),  $H_{1z}(r_0, k)|_{k=0} = (2\pi J_0/c)i(-k_0)\varepsilon$ ,  $\varepsilon = (1/2)r_0^6(R_m k_0 \ln \sqrt{R_m k_0})^2$ ], while in the case of a flat plate the longitudinal component of  $\mathbf{H}$  is expressed by an analogous formula without the small factor  $\varepsilon$ . From this it is clear that a reduction of the effectiveness of the propulsion unit resulting from the finiteness of the dimensions is less in the cylindrical case than in the flat-plate model. Formally this is due to the difference between the functions  $\Phi(k)$  (3.3),  $\psi_0(k)$  (3.5) in the region  $k = 0$ . The function  $\psi_0(k)$  has in this region a sharp maximum with width  $\Delta k \sim \sqrt{R_m k_0}$ , where  $\psi_0(0) = 1/\sqrt{2R_m k_0}$ . In the case of the function  $\Phi(k)$  this maximum is rather blurred (width  $\sim \pi$  when  $r_0 \lesssim 1$ ), and the quantity  $\psi(0)$  itself is small in comparison with  $\psi_0(0)$  [this can be seen from the estimate  $\psi(0) = -r_0^3(R_m k_0/4) \ln(r_0 \sqrt{R_m k_0})$ , which holds for  $r_0 \sqrt{R_m k_0} \ll 1$ ].

Nevertheless, the conclusion drawn in [2] that a system with a constant current amplitude along the propulsion section has low effectiveness remains valid. Therefore, except for one example, we shall not give the results here. The assumption that the use of amplitude modulation is suitable from the energy point of view also remains valid.

Before turning to numerical results, we shall show that for the values of  $k_0$  we are interested in, the dimensionless quantities  $F_1(k_0, r_0, R_m, s)$ ,  $Q_1(k_0, r_0, R_m, s)$ , and  $\eta(k_0, r_0, R_m, s)$  are actually independent of

TABLE 1

$k_0$	$r_0=0,1$		$R_m^0=0,005,$ $r_0=\infty$		$k_0$	$r_0=0,1$		$R_m^0=0,005,$ $r_0=\infty$		
	$F_1 \cdot 10^2$	$\eta$	$F_1 \cdot 10^2$	$\eta$		$F_1 \cdot 10^2$	$\eta$	$F_1 \cdot 10^2$	$\eta$	
$s=0,2$	$\pi$	3,06	0,077	157,46	0,002	$\pi$	-0,336	-0,168	13,76	0,000
	$3\pi$	12,82	0,158	54,86	0,069	$3\pi$	0,962	0,481	6,66	0,146
	$5\pi$	13,42	0,178	23,76	0,099	$5\pi$	0,984	0,492	2,02	0,169
	$7\pi$	11,74	0,187	15,56	0,120	$7\pi$	0,814	0,407	1,15	0,205
	$9\pi$	9,96	0,191	11,68	0,136	$9\pi$	0,670	0,335	0,81	0,243
	$11\pi$	8,50	0,193	11,40	0,147	$11\pi$	0,560	0,280	0,63	0,280
	$13\pi$	7,34	0,195	7,88	0,155	$13\pi$	0,478	0,239	0,52	0,315
	$15\pi$	6,44	0,196	6,78	0,162	$15\pi$	0,416	0,208	0,44	0,347
$s=0,4$	$\pi$	0,796	0,089	66,72	0,001	$\pi$	-0,462	-0,387	7,24	0,000
	$3\pi$	4,92	0,300	22,70	0,114	$3\pi$	0,522	0,406	4,80	0,138
	$5\pi$	5,12	0,349	9,28	0,161	$5\pi$	0,512	0,602	1,21	0,137
	$7\pi$	4,46	0,368	5,96	0,200	$7\pi$	0,410	0,693	0,62	0,152
	$9\pi$	3,76	0,378	4,44	0,230	$9\pi$	0,326	0,746	0,41	0,175
	$11\pi$	3,20	0,384	3,56	0,255	$11\pi$	0,266	0,779	0,30	0,201
	$13\pi$	2,76	0,388	2,96	0,274	$13\pi$	0,224	0,803	0,24	0,227
	$15\pi$	2,42	0,390	2,56	0,289	$15\pi$	0,192	0,819	0,20	0,254
$s=0,6$	$\pi$	0,04	0,012	32,38	0,001	$\pi$	-0,564	-0,640	1,87	0,000
	$3\pi$	2,28	0,412	11,96	0,144	$3\pi$	0,170	0,236	3,37	0,124
	$5\pi$	2,36	0,504	4,44	0,188	$5\pi$	0,142	0,400	0,57	0,085
	$7\pi$	2,02	0,540	2,76	0,235	$7\pi$	0,086	0,458	0,19	0,064
	$9\pi$	1,70	0,558	2,02	0,277	$9\pi$	0,050	0,478	0,09	0,052
	$11\pi$	1,44	0,569	1,60	0,313	$11\pi$	0,032	0,481	0,05	0,044
	$13\pi$	1,24	0,576	1,33	0,343	$13\pi$	0,020	0,480	0,03	0,039
	$15\pi$	1,09	0,581	1,14	0,369	$15\pi$	0,015	0,490	0,02	0,034

$R_m$  (when  $R_m \ll 1$ ), and consequently also independent of  $R_m^0$ . To do this, we shall expand the function  $\Phi(k)$  in powers of the small parameter  $R_m$ ; the first nonzero term of this expansion has the form

$$\Phi(k) = R_m \Phi_1(k), \quad \Phi_1(k) = \frac{r_0^2}{2} \frac{k_0 - ks}{|k|} I_1^2(|k|r_0) \{ |k|r_0 [K_0^2(|k|r_0) - K_1^2(|k|r_0)] + 2K_0(|k|r_0) K_1(|k|r_0) \}. \quad (3.6)$$

Equations (3.6) are valid for  $|k| \gg \sqrt{R_m k_0}$ , but in the region  $|k| \lesssim \sqrt{R_m k_0}$  they do not describe the function  $\Phi(k)$  (at the point  $k = 0$  they even have a logarithmic singularity). Therefore it is not permissible in the general case to use (3.6) as  $\Phi(k)$  in the integrals of (3.2). However, for those fixed values of  $k_0$  for which we have local maxima of  $\eta$  for the system under consideration, the position of the maximum of the function  $\Phi(k)$  (i.e., the point  $k \approx 0$ ) coincides with one of the zeros of the function  $i(k - k_0)$ ; the presence of the factor  $|i(k - k_0)|^2$  makes the integrals of (3.2) insensitive to errors in the formulation of the function  $\Phi(k)$  in the small interval  $|k| \lesssim \sqrt{R_m k_0}$  and enables us to use (3.6) as our  $\Phi(k)$ . Consequently we have proved the above proposition.

Now let us turn to the numerical results obtained by using amplitude modulation with  $i_0(z) = \cos \pi z$ . In this case the values of  $k_0$  which yield local maxima of  $\eta$  are equal to  $3\pi, 5\pi, 7\pi, \dots$  (actually they differ slightly from these values, but the differences are not worth taking into consideration).

The main results of the calculations are shown in the form of a table and graphs. In Fig. 2  $\eta$  is shown as a function of  $k_0$  for different values of  $s$  when  $r_0 = 0.25$ . The actual curves would be nonmonotonic (sawtooth) curves with local maxima at odd multiples of  $\pi$ , analogous to [2]. Since we are interested in precisely these regimes with maximum efficiency, the graphs given here are constructed for values of  $\eta$  (shown by dots in the graphs) calculated only for  $k_0 = \pi, 3\pi, \dots, 15\pi$  and are meaningless in the intervals between these values. Only for the case  $s = 0.6$  is the function  $\eta(k_0)$  shown as a broken line constructed by taking account of even multiples of  $\pi$ , for which  $\eta$  takes on minimum values. [These values were calculated from the general formulas (3.2) for  $R_m^0 = 0.005$ ; the stipulation of the value of  $R_m^0$  is necessary, since for these values of  $k_0$  the quantity  $\eta$  will depend on  $R_m$ .] Here, for comparison, we have shown by a dashed curve the result for a constant amplitude and shown by a dot-and-dash curve the result for the case  $r_0 = \infty, i_0(z) = \cos \pi z$ , also obtained for  $R_m^0 = 0.005, s = 0.6$ .

From the curves shown it can be seen that the use of amplitude modulation is indeed preferable, that as  $k_0$  increases the quantity  $\eta$  in the cylindrical geometry reaches its limiting value  $s$  much more rapidly than for  $r_0 = \infty$  (see also Table 1), and that the height of the teeth in the graph of  $\eta(k_0)$  in this geometry is much less than the corresponding quantity for  $r_0 = \infty$ . Lastly, the efficiency of the cylindrical system with a constant amplitude is also higher than in the analogous case of a flat plate. All of these features are due to the above-mentioned difference between the functions  $\Phi(k)$  and  $\Phi_0(k)$  in the region  $k = 0$ .

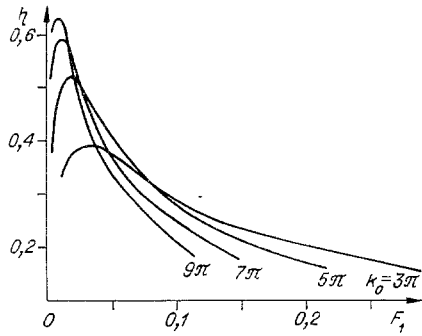


Fig. 3

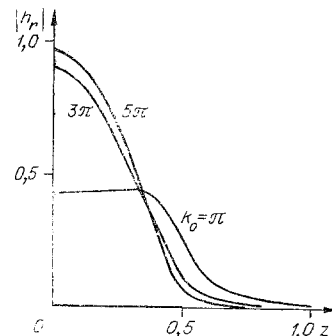


Fig. 4

To characterize the effectiveness of the propulsion unit, in addition to the function  $\eta(k_0)$  we must also give the dimensionless force  $F_1$ , which determines the value of the field required for creating the necessary thrust. In [2] the quantity  $F_1$  is given as a function of  $k_0$  for fixed  $s$  values. However, it seems more convenient to show on our graphs the function  $\eta(F_1)$  for fixed values of  $k_0$  (yielding local maxima of  $\eta$ ), obtained by eliminating  $s$  from the functions  $\eta(k_0, s)$ ,  $F_1(k_0, s)$ . The results relating to the case  $r_0 = 0.25$  are shown in Fig. 3. From this it can be seen that for large values of  $F_1$  (i.e., when the necessary thrust is attained for relatively small values of  $H_0$ ), we obtain small values of efficiency, and here it is most advantageous to use a system with  $k_0 = 3\pi$ . As  $F_1$  decreases, the  $\eta$  values attained increase, and in order to obtain the largest value of  $\eta$  we must pass to larger values of  $k_0$ . For example, in the interval  $F_1 = (0.03-0.06)$  it is preferable to have  $k_0 = 5\pi$ , in the interval  $F_1 = (0.0015-0.0025)$  it is preferable to have  $k_0 = 7\pi$ , etc. The curves given here are characteristic. The results for other values of the parameters, from which we can construct analogous graphs, are given in Table 1. From the table and the graphs it can be seen that the qualitative peculiarities of a cylindrical MHD propulsion unit are analogous to those obtained on a flat-plate model. However, taking account of the cylindrical shape involves substantial quantitative corrections, which improve the integral energy characteristics, and it is therefore necessary to take the shape into consideration.

5. A remark should be made concerning the use of the quantity  $2\pi J_0/c$  as the scale  $H_0$  of magnetic field intensity in the liquid. At first glance it appears that the "working" component  $H_r$  of the magnetic field outside the "solenoid" of finite length fed by the currents (1.1) must be small in comparison with  $H_0$ . Actually, although such an assumption is valid for a usual solenoid whose current density is constant along its length, it is not valid for the case under consideration here, in which along the length of the "solenoid" we can fit  $k_0/\pi$  half-waves of the current (1.1). In Fig. 4 we show the distribution of the amplitude of the field  $H_0$  at the boundary  $r = r_0$  along the cylinder for the case  $i_0(z) = \cos \pi z$ ,  $R_m^0 = 0.02$ ,  $r_0 = 0.25$ ,  $s = 0.2$ . Here the ordinate axis shows the modulus  $|h_r(z)|$  of the quantity  $h_r(z)$ , which determines the distribution

$$H_r|_{r=r_0} = \frac{2\pi J_0}{c} \operatorname{Re} h_r(z) e^{-i\omega_0 t}$$

[ $h_r(z)$  is calculated on the basis of (2.1), (2.2)]. It can be seen from the graphs that beginning with  $k_0 = 3\pi$ , the distribution of  $|h_r(z)|$  within the limits  $|z| \leq 1/2$  of the propulsion section is not very different from  $|i_0(z)|$ , and thus the quantity (3.4) does in fact characterize the true scale of the field in the liquid. Beyond the limits of the propulsion segment the field  $H$  damps out rapidly, and the larger  $k_0$  is, the faster the damping takes place.

6. In conclusion, we shall show by an example how the results given in Fig. 3 can be used. Suppose that the dimension of the propulsion section is  $a = 25$  m,  $r_0 = 0.25$ ,  $R_m^0 = 0.005$ . We calculate the quantity  $H_0$  required to create a specified thrust. From (3.1) we have  $|\langle F_Z \rangle| \approx 63.5 H_0^2 F_1$  (here the force is given in tons and  $H_0$  is given in teslas). Thus, if  $F_1 = 0.04$ , then the required field for creating a thrust, say, of 100 tons is  $\sim 6.3$  T. As can be seen from Fig. 3, we attain a value of  $\eta \sim 0.44$  if  $k_0 = 5\pi$ .

Corresponding to the values  $\sigma = 5 \cdot 10^{10} \text{ sec}^{-1}$ ,  $a = 2.5 \cdot 10^3 \text{ cm}$ ,  $u_0 = (9/\pi) \cdot 10^3 \text{ cm/sec}$  (where  $R_m^0 = 0.005$ ),  $H_0 = 6.3 \cdot 10^4 \text{ G}$ ,  $\rho = 1 \text{ g/cm}^3$  we have a magnetohydrodynamic interaction parameter  $N = \sigma H_0^2 a / \rho c^2 u_0$  equal to 0.19. Consequently, the assumption made here that the electromagnetic volumetric vortex forces have little effect on the field of velocities in the liquid can still be considered valid.

#### LITERATURE CITED

1. O. M. Phillips, "The prospects for magnetohydrodynamic ship propulsion," J. Ship Res., 5, No. 4 (1962).

2. V. I. Yakovlev, "On the theory of an inductive MHD propulsion unit with a free field," Dokl. Akad. Nauk SSSR, 249, No. 6 (1979); Zh. Prikl. Mekh. Tekh. Fiz., No. 3 (1980).

TRANSFORMER COUPLING OF INDUCTIVE AND RESISTIVE  
LOADS TO A MAGNETIC CUMULATION GENERATOR

A. S. Kravchenko, R. Z. Lyudaev,  
A. I. Pavlovskii, L. N. Plyashkevich,  
and A. M. Shuvalov

UDC 538.4:621.31

Magnetic cumulation (or explosive magnetic) generators are promising as high-power pulsed electrical energy sources [1-3]. When the load is connected directly into the circuit of the magnetic cumulation generator (MCG), the latter can operate efficiently only if restrictions are imposed on the inductance and resistance of the load, whereas in many applications the load parameters substantially exceed the inductance and resistance of the MCG, and the required time for energy input to the load may differ substantially from the general working time. One of the ways of matching the MCG parameters to the load is to use a stepup transformer [1]. Some designs of MCG with transformers have been described [3-7], with discussions of the matching of MCG to resistive and inductive loads. Some applications of transformer MCG in physics research have been discussed in [8-10].

Here we consider forms of transformer output from MCG to inductive and resistive loads. An electro-technical model is convenient for engineering calculations on transformer MCG, as supplemented with the experimental fact that there is an energy-optimal finite inductance for the generator.

1. In the electrotechnical model, the operation of the MCG is described by a series RL circuit with variable inductance  $L$  and resistance  $R$ , which formally includes all the losses of magnetic flux  $\Phi$ . Then  $I = \varphi \Phi_0 / L$ , where  $I$  is the current in the generator and  $\varphi = \exp\left(-\int_0^t \frac{R}{L} dt\right)$ , while the subscripts 0 and f denote the values of quantities, respectively, at the start and end of the operation of the MCG. If  $|dL/dt| > R$ ,  $I$  increases, while the magnetic energy  $W$  increases if  $|dL/dt| > 2R$ . If  $L_f \rightarrow 0$  when these conditions are met, then  $I_f \rightarrow \infty$ , which lacks physical meaning, and in that case the problem falls outside the framework of the electrotechnical model. In practice there is some minimum permissible value  $L_f$  for each generator.

Figure 1 shows the equivalent electrotechnical scheme for an MCG with a transformer working into a resistance  $R_l$  and inductance  $L_l$  with switch  $K$  closed and constant  $L_2$  and  $R_2$ , which is described by the system of equations

$$d(L_1 I_1)/dt + R_1 I_1 + L_{12} dI_2/dt = 0; \quad (1.1)$$

$$L_2 dI_2/dt + R_2 I_2 + L_{12} dI_1/dt = 0, \quad (1.2)$$

where  $L_1 = L_g + L_{1t}$ ,  $L_g$  is the working inductance of the MCG,  $L_{1t}$  is the inductance of the primary winding of the transformer, which includes  $L_c$ , the inductance of the current lead from the MCG to the transformer;  $L_2 = L_l + L_{2t}$ ,  $L_{2t}$  is the inductance of the secondary winding in the transformer;  $L_{12} = k(L_{1t} L_{2t})^{-1/2}$ ,  $L_{12}$  is the mutual inductance,  $k$  is the transformer coupling coefficient on the basis of  $L_c$ , while  $R_1$  and  $R_2$  are the circuit resistances, and  $R_l$  appears in  $R_2$ .

If  $R_2 = 0$  we have from (1.1) and (1.2) that

$$I_1 = \varphi_e \Phi_0 / L_e, \quad I_2 = -I_1 L_{12} / L_2 + I_{10} L_{12} / L_0 + I_{20},$$

where

$$L_e = L_1 - L_{12}^2 / L_2; \quad \Phi_0 = I_{10} (L_0 - L_{12}^2 / L_2); \quad \varphi_e = \exp\left(-\int_0^t \frac{R_1}{L_e} dt\right);$$

Moscow. Translated from Zhurnal Prikladnoi Mekhaniki i Tekhnicheskoi Fiziki, No. 5, pp. 116-121, September-October, 1981. Original article submitted August 5, 1980.